

## THE GROUND-BASED EUROPEAN NULLING INTERFEROMETRY EXPERIMENT (DARWIN-GENIE)

P. Gondoin, O. Absil, R. den Hartog, L. Kaltenecker, C. Eiroa, C. Erd  
M. Fridlund, A. Karlsson, A. Peacock, Z. Sodnik, S. Volonte<sup>1</sup> and  
R. Wilhelm, M. Schoeller, A. Glindemann<sup>2</sup>

<sup>1</sup>European Space Agency, P.O. Box 299, 2200AG Noordwijk, The Netherlands ,

<sup>2</sup>European Southern Observatory, D-85748 Garching bei Munchen, Germany

### ABSTRACT

Darwin is one of the most challenging space projects ever considered by the European Space Agency (ESA). Its principal objectives are to detect Earth-like planets around nearby stars and to characterise their atmospheres. Darwin is conceived as a space “nulling interferometer” which makes use of on-axis destructive interferences to extinguish the stellar light while keeping the off-axis signal of the orbiting planet. Within the frame of the Darwin program, the European Space Agency (ESA) and the European Southern Observatory (ESO) intend to build a ground-based technology demonstrator called GENIE (Ground based European Nulling Interferometry Experiment). Such a ground-based demonstrator built around the Very Large Telescope Interferometer (VLTI) in Paranal will test some of the key technologies required for the Darwin Infrared Space Interferometer. It will demonstrate that nulling interferometry can be achieved in a broad mid-IR band as a precursor to the next phase of the Darwin program.

Key words: Darwin; groundbased interferometry; nulling interferometry.

### 1. INTRODUCTION

Understanding the principles and processes that created the Earth, and allowed the development and evolution of life forms to take place is a key scientific objective which has been brought as a very high priority to the attention not only of the European Science Community but also of the European Space Agency. In particular, the successful detection of Earth-like planets possessing environments benign to life would answer central questions such as “How unique is the Earth as a planet ?” and “How unique is life in the Universe ?”. To achieve these objectives, the Darwin mission of the European

Space Agency (Fridlund 2000; Fridlund & Gondoin 2002) will survey a large sample of nearby stars and search for Earth-size planets within their “habitable zone”. Darwin will measure their spectra in order to infer the presence of an atmosphere and search for biomarkers.

Detection of Earth-size bodies circling nearby stars is extremely difficult because of the weak planetary signal emitted within a fraction of an arcsecond from an overwhelmingly bright star. A solar type star outshines an Earth size planet by a factor of more than  $10^9$  in the visible wavelength range (see Fig.2). In the infrared spectral range, where the planet’s thermal emission increases and the star’s emission decreases, the contrast is still higher than  $10^6$ . Only the planetary signal, a millionth of the stellar light, should remain in the input feed of a spectrograph in order to register a planet spectrum in a reasonable time. To accomplish such an extinguishing of light at the relevant spatial scales, the technique of “nulling interferometry” has been selected for Darwin. By applying suitable phase shifts between different telescopes in an interferometric array, destructive interference can be achieved on the optical axis of the system in the combined beam while interference is constructive for small off-axis angles. The principle of nulling interferometry for a simple two telescope Bracewell interferometer (Bracewell 1978) is described in Fig. 1. The equivalent transmission map of the nulling interferometer is a set of interference peaks with a sharp null in the centre. By placing the central star under this null, and adjusting the interferometer baseline to the required angular resolution, planets can be detected in the “habitable zone”. The actual shape and transmission properties of the pattern around the central null depend on the configuration and the distance between the telescopes.

The Darwin mission concept (ESA 2000) consists of six 1.5 m telescopes, each of which is a free flying spacecraft transmitting its light to a central beam-combining unit (see Fig. 3). Using the nulling interferometry technique, the beam combiner extinguish the stellar light by destructive interferences

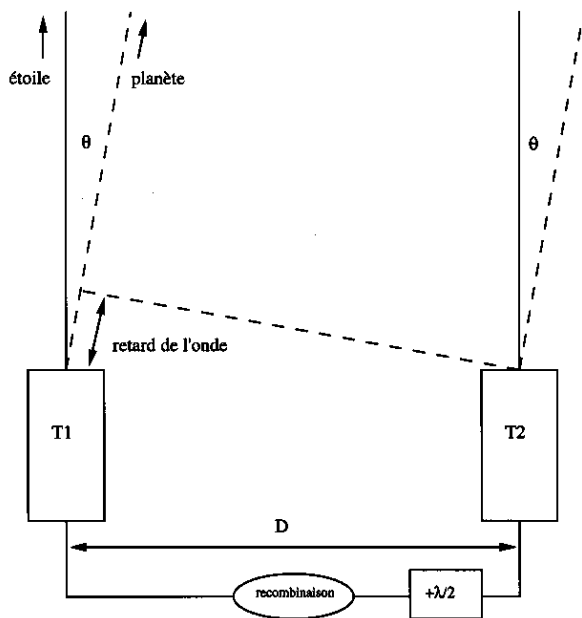


Figure 1. Principle of a two telescopes Bracewell interferometer.

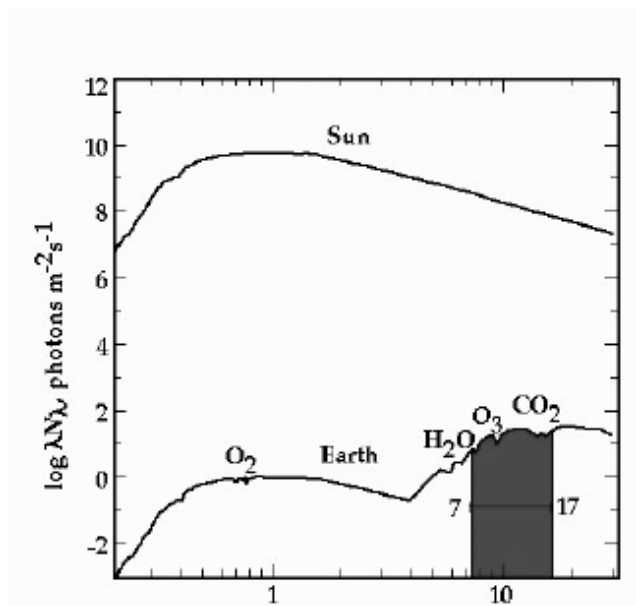


Figure 2. Contrast between the solar flux and the Earth as a function of wavelength in microns. Adapted from Angel et al. (1986).

on-axis and transmit the off-axis signal of the orbiting planet. The light from Earth-like planets at interstellar distances of up to 25 parsecs can then be analysed. The mission concept is based on the ability to co-phase telescopes on independent spacecrafts to an accuracy better than 20 nm and to perform nulling interferometry with a rejection factor of  $\approx 10^5$  in a wide spectral band extending from 5 to 18  $\mu\text{m}$ . In-orbit co-phasing of the free-flying telescopes is performed in successive steps combining first a local radio-frequency positioning system with milli-Newton propulsion devices, then inter-satellite laser metrology with micro-Newton propulsion devices and finally fringe sensors with optical delay lines. These items are currently developed within the ESA Technology Research Program (TRP). It is envisaged to test them in-orbit within the frame of the ESA SMART technology demonstration program.

In addition to the co-phasing of free-flying telescopes, a second key issue for Darwin is the nulling interferometry technique. Hence, the TRP activities also include the development of Darwin specific optical components, namely achromatic phase shifters, wavefront filtering devices and IR single mode fibres, integrated optics, IR detectors, electronics and coolers, optical delay lines and fringe sensors as well as other components for interferometry. Laboratory nulling breadboards with star-planet simulators are currently evaluating the performance of the nulling interferometric technique (Barillot 2003; Flatscher 2003). These innovative breadboards use the narrow telecommunication band around 1.65  $\mu\text{m}$  where off-the-shelf components are available. Based on their performance, a follow-up activity has been identified which will adapt their design to the mid-IR band and test the nulling interferometry technique on astronomical targets in Darwin representative operating conditions. The Very Large Telescope Interferometer (VLTI; Schöller & Glindemann 2003) at the European Southern Observatory (ESO) is the most appropriate infrastructure on-ground to perform such a test. Hence, ESA and ESO initiate a definition study for a Groundbased European Nulling Interferometry Experiment which will operate in the central laboratory of the VLTI at Mount Paranal (Chile). This experiment is called Darwin-GENIE. The definition study will assess the technical feasibility of the experiment and establish its design, performance, programmatics and cost. If successful, the definition study will be the base for ESA and ESO to move into the hardware development, integration and exploitation phases of the GENIE project.

## 2. GENIE OBJECTIVES

### 2.1. Demonstration of Darwin technology

The primary objective of the Darwin-GENIE nulling experiment (Gondoin et al. 2003) is to gain experience on the design, manufacture and operation of a nulling interferometer using Darwin representative



Figure 3. Artist view of the Darwin Space Interferometer orbiting at Sun-Earth L2 point (courtesy Alcatel Space Division).



The VLTI Array on the Paranal Mountain

ESO PR Photo 15a/00 (24 May 2000)

© European Southern Observatory



Figure 4. The ESO Very Large Telescope Interferometer with its four 8.2 meter telescopes and its central interferometric laboratory.

concept and technology. Nulling tests with the highest rejection factor on single stars or close binaries in broad mid-IR spectral bands will achieve this objective with the limitations imposed by the turbulence and infrared background of the Earth atmosphere. The Darwin-GENIE experiment will combine all optical functions foreseen into the future Darwin Infrared Space Interferometer. It will benefit from the existing VLTI infrastructure, including the telescopes with chopping and adaptive optics, the delay lines, the fringe sensors and the beam combiner laboratory. The overall performance of the instrument will heavily depend on the performance of all VLTI subsystems and in particular on the adaptive optics and co-phasing subsystems. The GENIE optical bench within the VLTI laboratory will provide the functions specific to the nulling interferometry technique, namely photometry and amplitude control, polarization matching, phase shifting, beam combination and internal modulation, spatial filtering, spectrometry, detection, electronics and cryogenics. The detailed architecture of Darwin-GENIE will be established during the definition study. It will take into account the ESO VLTI interface characteristics and the output of the ESA TRP activities.

## 2.2. Preparation of the Darwin science program

Darwin science program aims to detect Earth-like planets around nearby stars, to determine their characteristics, to analyse the composition of their atmospheres and to assess their ability to sustain life as we know it. An important information for a proper design of the direct planet detection experiment of Darwin is the frequency of Earth-like planets around G, K and M dwarfs. The COROT, Eddington and Kepler space missions will detect massive bodies around cool stars by occultation and will thus provide this information. These missions are thus to be considered as true precursors to Darwin. A second objective of GENIE is also to prepare the Darwin science program through a systematic survey of Darwin candidate targets (Eiroa et al. 2003). The solar zodiacal cloud, a sparse disk of 10–100  $\mu$  diameter silicate grains, is the most luminous component of the solar system after the Sun. Its optical depth is only  $\approx 10^{-7}$ , but a patch of the solar zodiacal cloud 0.3 AU across has roughly the same emitting area as an Earth sized planet. Similar and even brighter clouds may be common in other planetary systems and present a severe obstacle for the direct detection of extra-solar terrestrial planets. A systematic survey of Darwin candidate targets will screen-out those stars for which circumstellar dust prevent the detection of Earth-like planets. Bright exozodiacal clouds are easier to detect than extra-solar terrestrial planets, but finding an exozodiacal cloud is still difficult. The total emission from our zodiacal cloud is no more than  $10^{-4}$  of the Sun's at any wavelength. Photometric surveys like the Infrared Astronomical Satellite (IRAS) survey can only detect exozodiacal clouds that are  $> 500$  times as optically thick as the solar clouds (Backman & Parece 1993). Attempts to

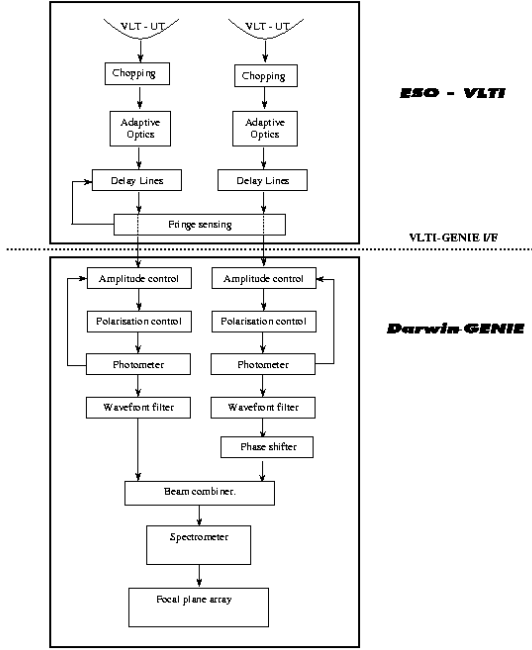


Figure 5. Functional description of GENIE.

spatially resolve faint exozodiacal clouds with single-dish telescopes in the mid-infrared and near infrared (Küchner & Brown 2000) have not yielded better detection limits. A Bracewell interferometer using two ESO VLTI 8m Unit Telescopes (UT) could provide better performance.

### 3. THE BRACEWELL INTERFEROMETER: A POSSIBLE CONFIGURATION FOR GENIE

The transmission map  $T(\theta, \phi)$  (see Fig. 6) of a diffraction limited Bracewell interferometer with two circular entrance apertures can be expressed as a function of wavelength, telescope diameter  $D$ , and projected baseline  $B$  as follows:

$$T(\theta, \phi) = 2 \times \frac{J_1(\pi\theta D/\lambda)}{\pi\theta D/\lambda^2} \times \sin^2(\pi\theta \cos(\phi)B/\lambda) \quad (1)$$

$\theta, \phi$  are respectively the angular distance to the bore-sight and the azimuth angle in the plan of the sky with respect to the projected baseline. Eq.(1) assumes a diffraction limited operation without any residual wavefront error, with a perfect  $\pi$  phase shift between the two arms of the interferometer and equal amplitudes of the recombining fields. In practice, the central null of the transmission map will be degraded

by amplitude and optical path differences (OPD) between the two arms of the interferometer that are not perfectly corrected.

Also, wavefront distortions induced by atmospheric turbulence will only be partially compensated by the adaptive optics. Spatial filtering of the high frequencies wavefronts errors by monomode optical fibres or waveguides will be required (Ollivier & Mariotti 1997). The coupling efficiency in the fibre will be variable (Shaklan & Roddier 1988) depending on the fluctuating wavefront and pointing errors. Hence, the envelope of the transmission map of the interferometer will significantly depart from a Bessel function and will be highly time variable. In the Gaussian approximation, the optimum injection efficiency into a fibre is found for an aperture ratio such that the diffraction limited image has approximately the size of the core (Ruilier 1998). The geometrical extent of the beam seen by the fibre is then  $S\Omega \approx \lambda^2$ . The IR thermal background contribution is then proportional to  $S\Omega \approx \lambda^2$  while the signal included into the field-of-view of the interferometer is proportional to the collecting area. Hence, the ratio signal to noise of an exozodiacal dust cloud observed in the mid-IR by a Bracewell interferometer is proportional to its collecting area and the largest telescopes shall be used.

The output signal of a Bracewell interferometer pointing to a star surrounded by a dust cloud can be expressed as follows:

$$S(\theta, \phi) = A_{\text{eff}} \int_{\theta} \int_{\phi} T(\theta, \phi) O(\theta, \phi) d\theta d\phi + Bgd \quad (2)$$

where  $T(\theta, \phi)$  is the transmission map of the interferometer degraded by residual amplitude fluctuations and optical path differences between the two interferometer arms.  $O(\theta, \phi) = O_s(\theta, \phi) + O_z(\theta, \phi)$  is the sum of the brightness of the star and of the exozodiacal dust disk.  $Bgd$  is the incoherent background signal which includes the thermal emission from the sky and from the telescope and instrument optics.

Since the only reliable observations on zodiacal dust have been carried out in the solar system, spectral properties of the exozodiacal dust emission can only be extrapolated from observations of the solar interplanetary dust cloud performed by the Diffuse Infra-Red Background Experiment (DIRBE) on board the COBE satellite. A comprehensive dust disk model is due to Kelsall et al. (1998) who express the dust density  $n(r, z)$  as the product of a radial power law term and a vertical decreasing exponential term, i.e  $n(r, z) = n_0 \times r^{-\alpha} \times f(z/r)$ . A disk inner cut-off is assumed to account for the sublimation of dust grain close to the star at temperatures higher than about 1500 K. Since the contribution of the scattered stellar light is negligible in the infrared, the brightness of the cloud is expressed as an integral along the line of sight of the thermal emission of the dust which temperature is a decreasing function of the distance  $r$  to

Table 1. Exozodiacal flux, star/cloud brightness contrast of an exo-zodiacal cloud 10 times denser the solar zodiacal dust and located around a G2 V star at 10 pc.

Spectral band	L'	N
Exo-zodiacal flux (mJy)	0.5	1.1
Magnitude	14.2	11.3
Star/cloud contrast	30000	2500

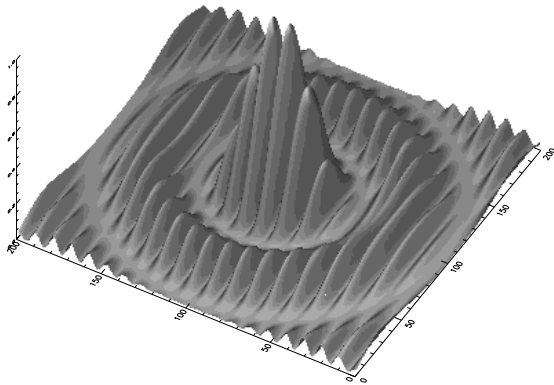


Figure 6. Transmission map of a diffraction limited Bracewell interferometer with circular entrance apertures.

the star. Eq.(1) indicates that the first maximum of the transmission map is located approximately at  $\theta = \lambda/(2 \times B)$ . The hot inner dust of nearby solar-like zodiacal clouds, which has a high density, will therefore most contribute to the overall signal registered with a 50 m baseline interferometer. Flux considerations indicate that both the L' band at  $3.8 \mu\text{m}$  and the N band around  $10.2 \mu\text{m}$  could be appropriate for the detection of exozodiacal dust clouds around nearby stars with two ESO VLT telescopes operating as a Bracewell interferometer. In principle, the M band could also be considered but can be highly affected by the presence of varying amounts of water vapour in the atmosphere. Table 1 shows the flux of an exozodiacal dust cloud 10 times denser than the solar zodiacal dust around a G2 V star at 10 pc. The contrast between the star and the dust cloud brightness is also given for the different atmospheric bands. The N band present a significant advantage over the L' band since the contrast between the star and the dust cloud is lower by a factor of 10.

## 4. THE TECHNICAL CHALLENGES

### 4.1. Minimization of the stellar leakage

The transmission map of a Bracewell interferometer exhibits a narrow null with a  $\theta^2$  transmission on axis. Eq. 2 indicates that the high spatial resolution of a two telescopes interferometer with a  $\approx 50$  m baseline does not completely reject the starlight on axis specially when stars are closer than 50 pc. A residual stellar signal  $S_{\text{leak}}$  leaks through the transmission map. It can be expressed as a function of the operating wavelength  $\lambda$ , interferometer baseline  $B$  and angular radius  $\theta_s$  of the star as follows:

$$S_{\text{leak}} = A_{\text{eff}} \int_{\theta} \int_{\phi} T(\theta, \phi) O_s(\theta, \phi) d\theta d\phi \quad (3)$$

i.e. for a diffraction limited Bracewell interferometer:

$$S_{\text{leak}} = A_{\text{eff}} \times O_s \times (\pi^2/8) \times (\theta_s B/\lambda)^2 \quad (4)$$

In practice the transmission map is distorted and fluctuating rapidly as a function of time. Unequal amplitudes between the arms of the interferometer affect the depth of the null. Variations of the optical path difference (OPD) between the two telescopes induce random displacements of the central dark fringe. Hence the null signal is fluctuating on time scale that are short compared with typical integration times. When averaged over the detector frame read-out time ( $f_{\text{ro}}^{-1}$ ), one major effect of the stellar leakage is to raise the depth of the null to an average stellar leakage  $\langle S_{\text{leak}} \rangle$  that can be estimated as follows:

$$\frac{\langle S_{\text{leak}} \rangle}{F_s \times f_{\text{ro}}^{-1}} = \frac{\alpha^2}{4} + \frac{4\alpha\Delta}{3\pi} + \left(\frac{\pi\sigma_{\text{piston}}}{\lambda}\right)^2 + \sigma_a^2 + \frac{\Delta^2}{4} \quad (5)$$

where  $\alpha = \frac{\pi\theta_s}{\lambda/B}$ .  $\sigma_a$  is the rms fluctuation of the relative amplitude between the two arms of the interferometer after spatial filtering.  $\sigma_{\text{piston}}$  is the rms fluctuation of the piston i.e the residual rms OPD fluctuation after correction by a delay line operated by a fringe sensor unit in a close loop system.  $\Delta$  is a phase shift residual depending on wavelength which describe dispersion effects. In addition to an average offset of the null depth, a major effect of the stellar leakage is to induce important noise contributions. One contribution is the photon noise of the mean stellar leak  $\langle S_{\text{leak}} \rangle$  which adds onto the photon noise of the background and of the exo-zodiacal dust clouds. This degrades the ratio signal to noise of the exo-zodiacal dust disk measurements (see Eq. 7). A second source of noise is the erratic fluctuation  $\sigma_{\text{leak}}$  of the stellar leakage due to residual variations at high frequencies of the amplitude and optical path difference between the two arms of the interferometer. The rms fluctuation of the stellar leakage are expressed as follows:

$$\sigma_{leak} = F_s \times \frac{8\alpha}{3\pi} \times \sqrt{\left(\frac{\pi\sigma_{piston}}{\lambda}\right)^2 + \sigma_a^2} \times f_{ro}^{-1} \quad (6)$$

The effect of the stellar leakage fluctuations and photon noise on the ratio signal to noise of the dust disk flux measurements can therefore be expressed as follows:

$$S/N = \frac{S_z \sqrt{\Delta\lambda\Delta t}}{\sqrt{Bgd + S_z + \langle S_{leak} \rangle + \sigma_{leak}^2}} \quad (7)$$

Nulling interferometers using three or four ESO VLT telescopes could provide theoretically a broader null and could be therefore less sensitive to stellar leakage. However, such configurations with three or four VLTs would be non-linear. The Earth rotation would induce a non-homothetic deformation of the projected bidimensional array on the plane of the sky, so that continuous amplitude adjustments would be needed to compensate the array deformation during the night and to maintain a broad  $\theta^4$  null. Additional engineering complexity would come from the increased number of fringe sensors and OPD control units. Furthermore, the stellar light leakage through groundbased nulling interferometer using more than two telescopes would be in practice much larger than their theoretical transmission due to their high sensitivity to residual OPD and Strehl amplitude fluctuations.

Photon noise and fluctuations of the stellar leakage are major limitations for the detection of exozodiacal dust clouds using a groundbased nulling interferometer. Eq.(4) shows that the stellar leakage of a Bracewell interferometer and therefore its contributions to the noise can be reduced by operating at long wavelength with short baselines. According to this criterion, the detection of exo-zodiacal dust clouds at VLTI would be most efficient with a Bracewell interferometer operating in the N band and combining two large 8.2 m UT telescopes with the shortest VLTI baselines (e.g 46 or 56 meters).

#### 4.2. Subtraction of the thermal IR background

In the N band, the infrared background flux in the interferometer field of view is about 300 times larger than the flux from a Sun-like star located at 10 parsecs. In order to measure a null depth of a few thousands, the background flux has to be subtracted with a high accuracy. In the L' band, the requirement on the background calibration accuracy is relaxed since the background flux is much smaller. The background thermal emission contributes to the noise not only by its photon noise but also by its temporal fluctuations. Eq. 7 assumes that chopping is efficient enough to remove background fluctuations. In practice, little is known about the stability of the background in the mid-IR both on long and short

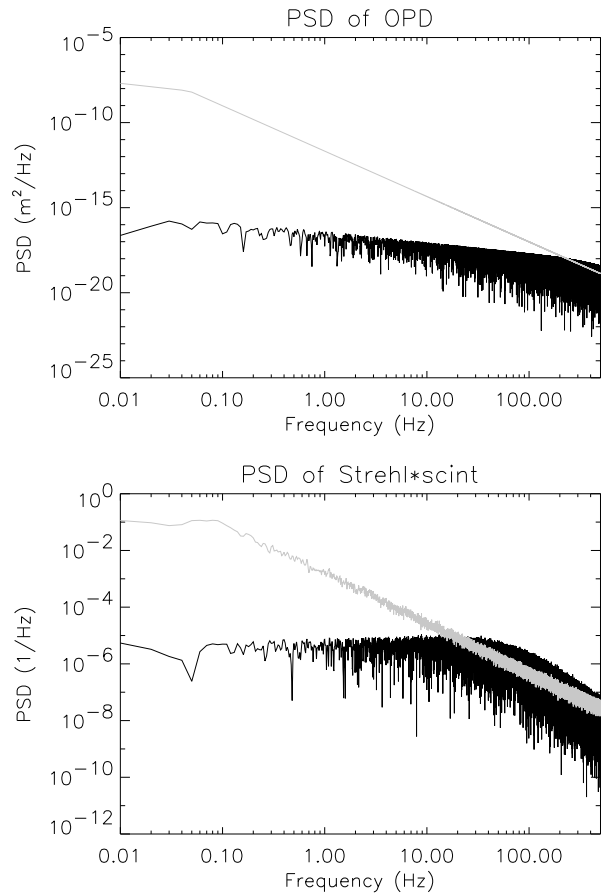


Figure 7. Simulation examples of the power spectral densities of the optical path difference (top) and Strehl fluctuations (bottom) before and after correction by OPD and amplitude control loops of the GENIE experiment.

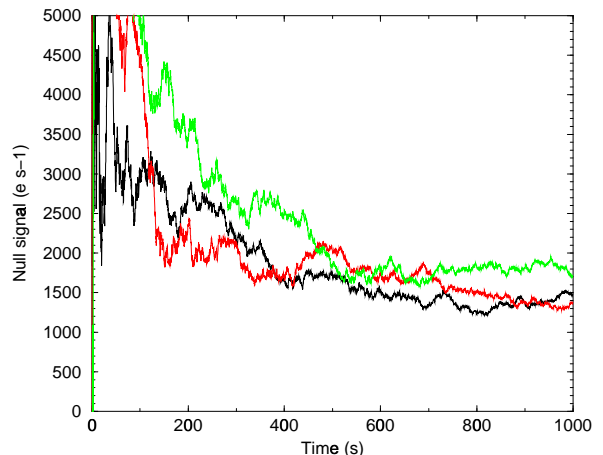


Figure 8. Geniesim simulation example of a cumulative averaged null signal in three different spectral channels.

time scales. The infrared sky noise in the N band is mainly due to aerosols and cirrus clouds, confined to the Earth's troposphere (Kaufl 1991). Its power spectrum has been measured by several authors in different infrared spectral bands (e.g. Miyata et al. 2000). These measurements show that the infrared background level and fluctuations greatly depends on the astronomical site (altitude, humidity, ...), on the sky condition at the moment of the observation and on the instrument and telescope, which contribute to a great extent to the infrared emission. Obtaining these information at Paranal is therefore crucial for designing the GENIE experiment. A measurement campaign of thermal infrared emission and atmospheric dispersion has been initiated (Wilhelm & Gilton 2003) which will benefit from the installation of the MID-Infrared instrument (MIDI; Leinert et al. 2003) at the ESO VLTI.

For background subtraction, GENIE could use the VLT chopping sub-system where the target and background are alternatively observed by tilting the VLT secondary mirrors. Since the background is not expected to be spatially uniform, the nodding technique could be applied. The main drawback of this chopping method is that the tip-tilt unit, the adaptive optics and the fringe sensor cannot remain in closed loops since they do not see the central guide star when measuring the background. All these sub-systems have to reclose their loops before each single interferometric measurement is made. The overall detection performance of GENIE will thus depend on the efficiency of these subsystems which are expected to close their loops in a few hundred milli-seconds, while a chopping period is expected to last typically for 100 msec. Alternative methods could improve this chopping efficiency. These include counter chopping of a control beam operating in a separate H or K band or a dual feed interferometer where one of the beam remains on the guide star to feed the subsystems. A third possibility is to use an internal chopping method similar to the one proposed in the context of the Keck nuller (Serabyn 2003). In this method, the exit pupils of each of two telescopes are divided in two parts. Each half-pupil of one telescope is recombined destructively with the corresponding half-pupil of the other telescope, such that two Bracewell interferometers with parallel baselines are formed. Their nulled output are then combined with a  $\pm\pi/2$  phase shift. Chopping can thus be carried out at high frequencies by alternately registering the signal from these two outputs.

Based on the result of IR thermal background measurement performed at Paranal, the definition study of GENIE will trade-off these different chopping methods and assess the feasibility of detecting exozodiacal dust clouds around nearby stars with a Bracewell interferometer. The thermal infrared background level is clearly a major obstacle for the study of exo-zodiacal dust clouds in the N band.

#### 4.3. Compensation of the atmospheric dispersion

A wideband interferometer such as GENIE is sensitive to the effect of longitudinal dispersion which affect the interfering light beams unequally. For infrared observations, this effect is due to the unbalanced air paths in the delay line and to random atmospheric humidity variations in the line-of-sight to the star and inside the VLTI delay line tunnels. Longitudinal dispersion determines the position of the null fringe as a function a wavelength, and is therefore a central problem in producing deep broadband interferometric nulls. It produces two deleterious effects, namely (i) an inter-band dispersion between the spectral band where the OPD is controlled and the measurement band where the null is achieved and (ii) an intra-band dispersion within the measurement band.

In the case of the VLTI, the PRIMA fringe sensor unit could be used to correct the differential OPD in the infrared K band. However, the different amounts of air and water vapour crossed by each light beam would lead to an offset of the dark fringe position in the L' or N band where GENIE will operate. Also, random fluctuations of water vapour content in the path of the beams will lead to a random motion of the dark fringe. This needs to be compensated e.g. by periodically measuring the fringe position in the L' or N band, or by monitoring the changing differential water column. Dry air has very little dispersion in the infrared. The amount of dry air-induced dispersion varies slowly with time as the delay lines are moved to compensate for Earth rotation. The refractive index of dry air can be fit fairly well with dispersive solids such as ZnSe. The correction of dry air dispersion is therefore relatively easy, e.g. by introducing an adjustable pathlength through ZnSe in one arm of the interferometer. Water vapour, on the contrary, has a strong dispersion in the infrared, and the column densities of water vapour above the telescopes can differ enough to contribute significantly (Meisner & Le Poole 2003). Moreover, the amount of water vapour in the two light paths varies randomly due to atmospheric turbulence. Therefore, the correction of water vapour dispersion is a more difficult task. ZnSe dispersion control devices combined with delay lines could still be used (Koresko et al. 2003) providing that a high degree of symmetry is kept in the nuller design to minimize unbalanced reflectivity, transmission or polarisation in the optical system. A pair of wedges is a candidate solution to adjust pathlength through ZnSe while keeping constant the direction of the beams.

## 5. GENIE NULLING PERFORMANCE

A simulation software has been developed (Absil et al. 2003a) in an IDL based code to simulate nulling tests and observation scenarios that could be conducted with the GENIE experiment. The code emulates the brightness distribution of the target source

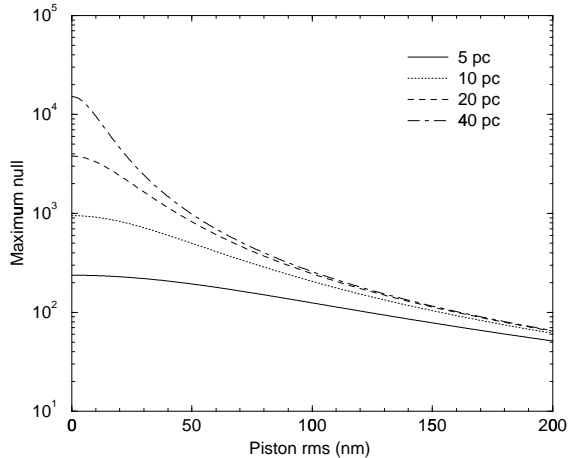


Figure 9. Maximum achievable rejection ratio in the L band as a function of the residual rms piston error for a G2 V star at 5, 10, 20 and 40 pc. A 46 m UTs telescope interferometer is assumed with a 46 meter baseline.

including the central star, its circumstellar dust disk and the eventual presence of a low-mass companion. The noise contribution from the thermal infrared emission of the atmospheric background and of the VLTI is added to the signal. A Kolmogorov power spectrum describes the effect of the atmospheric turbulence on the fluctuation of the optical path difference between the telescopes. The GENIE instrument is described by the transfer functions of its different subsystems. This includes the control loops of the MACAO adaptive optics and of the PRIMA fringe sensor unit of the ESO Very Large Telescope Interferometer. Examples of the power spectrum of the OPD and Strehl fluctuations are given in Figure 7 before and after filtering by the OPD control loop and amplitude matching subsystems of the experiment. The output signal of the GENIE simulator consists in time series of fluxes calculated in different spectral channels by folding the brightness distribution of the source with instantaneous transmission map of the GENIE experiment distorted by OPD, amplitude mismatch and background offsets. Examples of simulation results are given in Fig. 8 which show the cumulative averaged nulled signal after background subtraction in three different channels as a function of integration time. In this example a moderately stable null of about 1500 is achieved in a thousand second.

One major performance limitation of a Bracewell interferometer operating on nearby stars is due to starlight leakage through the transmission map. The results of a parametric performance analysis model are summarized in Figure 9. Fig. 9 gives the maximum achievable rejection ratio in the L band as a function of the residual rms piston error for a G2 V star at 5, 10, 20 and 40 pc in the L. A baseline of 46

meter is assumed between two UT telescopes. In the L band, the nulling performance are severely limited by stellar leakage for stars closer than 10 parsecs. For more distant stars, the maximum achievable null is rapidly dropping with the degradation of the OPD control accuracy. The OPD control loop is a major subsystem of the GENIE experiment and drives the nulling performance of the interferometer in the L band. This control loop includes a fringe sensor unit and a delay line. Its performance depends on the power spectral density of the OPD induced by atmospheric turbulence, on the residual fringe motion over the FSU integration time, on the photon flux available from the celestial object and on its visibility factor. The presence of a bright star in the center of the field of view of a nulling interferometer enable to control the optical path difference between the two arm of the interferometer with an accuracy high enough to achieve a nulling depth greater than a thousand.

In order to avoid a degradation of the nulling performance by the wavefront errors, GENIE will use monomode optical fibers or waveguides. These devices will filter the high order wavefront errors that will remain after correction by the VLTI adaptive optics subsystem. Hence, the coherent flux used for destructive interference can be assumed to be the fraction of the total flux equal to the Strehl ratio. The Strehl ratio is expected to fluctuate rapidly due to atmospheric turbulence, therefore affecting the nulling performance. The amplitude fluctuation will have to be corrected by an amplitude matching device. A proper correction will be achieved providing that the error signal, i.e. the instantaneous filtered intensity of the star, can be measured with a ratio signal to noise consistent with the required amplitude matching accuracy. With an integration time too short, the Poisson statistics will prevent to achieve the measurement accuracy. If the photometric integration time is too long, fluctuations of the instantaneous stellar signal within the integration time will exceed the required amplitude matching accuracy. Table 2 and 3 quantify the effect of rms OPD variations, rms

Table 2. Effect of RMS OPD fluctuations, amplitude fluctuation and thermal infrared background noise on the nulling depth and ratio signal to noise of the stellar leakage measurement. A 100 seconds nulling test is assumed on a A0 V star located at 50 parsecs. Only one spectral channel of  $1 \mu\text{m}$  width centered at  $3.8 \mu\text{m}$  in the L' band is considered assuming no performance degradation by dispersion effect.

$\sigma_{opd}$ (nm)	$\sigma_{amp}$ (%)	bckgd ( $e^- s^{-1}$ )	Null	S/N
0	0	0	2290	1570
0	0	$9.7 \times 10^6$	2290	79
0	2.5	0	1690	60
20	0	0	1980	77
20	2.5	0	1510	56
20	2.5	$9.7 \times 10^6$	1510	50

amplitude fluctuations and thermal infrared background noise on the nulling depth and ratio signal to noise of the stellar leakage measurement. In the N band (Table 3), a 1 hour nulling test is assumed on a G2 V star located at 10 parsecs. In the L' band, a 100 seconds nulling test is considered on a A0 V star located at 50 parsecs. A spectral channel width of  $1 \mu\text{m}$  has been used in the calculation assuming no performance degradation by dispersion effects. Fluctuation of the thermal infrared background emission are not taken into account. Table 2 and 3 indicate that an amplitude control with a percent accuracy is sufficient to maintain a nulling rejection ratio larger than a 1000. It is anticipated that such a performance will be easily achievable in the L' band but more difficult to obtain in the N band due to the high level of the thermal background emission and due to its fluctuations.

Nulling performance in the N band are less sensitive to residual OPD fluctuations due to the longer operating wavelength. Fig. 10 (top) estimates the nulling performance of the GENIE instrument with a 46 m baseline in the N band as a function of the star distance and spectral type assuming an OPD control accuracy comparable to that achieved with the VLTI PRIMA fringe sensing unit. A nulling rejection factor greater than a thousand is obtained for dwarf M, K or G stars at distance greater than 5 parsecs. However, due to the high level of the thermal infrared background, the integration time needed to measure the nulling rejection ratio at a  $3 \sigma$  accuracy level rapidly increases with distance. Fig. 11 shows that hours of integration will be needed to measure the stellar leakage at a rejection level of 1600–1800 on G–K dwarfs at 20 pcs and M dwarfs within 10 pcs. This estimate does not take into account additional performance limitation due sky background fluctuations and atmospheric dispersion that will be difficult to correct in the N band. The L' band is considered as an alternative operation band for the GENIE ground based nulling demonstrator despite its tighter requirement on the OPD control accuracy.

*Table 3. Effect of RMS OPD fluctuations, amplitude fluctuation and thermal infrared background noise on the nulling depth and ratio signal to noise of the stellar leakage measurement. A 1 hour nulling test is assumed on a G2 V star located at at 10 parsecs. Only one spectral channel of  $1 \mu\text{m}$  width centered at  $10.2 \mu\text{m}$  is considered assuming no performance degradation by dispersion effect. Thermal infrared background fluctuations are not taken into account.*

$\sigma_{opd}$ (nm)	$\sigma_{amp}$ (%)	bckgd ( $e^- s^{-1}$ )	Null	S/N
0	0	0	3810	2610
0	0	$4.4 \times 10^9$	3810	4
0	2.5	0	2390	325
100	0	0	2000	315
100	2.5	0	1520	322
100	2.5	$4.4 \times 10^9$	1520	4

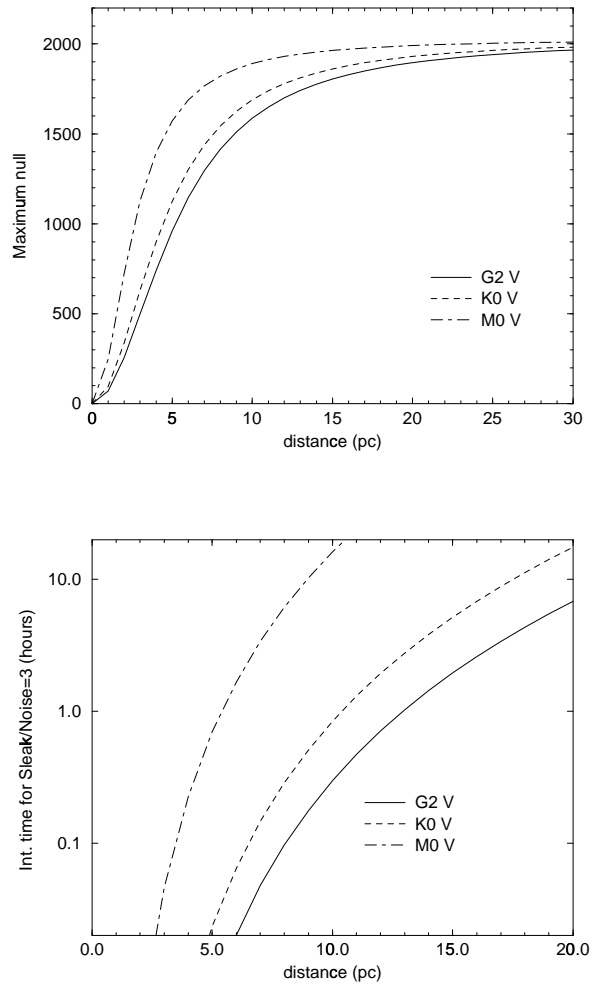


*Figure 10. Maximum achievable null (top) in the N band as a function of star distances and spectral types assuming an OPD control accuracy similar to the ESO VLTI PRIMA fringe sensor unit. Nulling performance better than 1000 can easily be achieved. However, due to the strong thermal infrared background, the integration time (bottom) needed for a null depth measurement at a  $3 \sigma$  level accuracy in the N band increases rapidly with the target distance.*

## 6. DARWIN-GENIE: A GENERAL USER INSTRUMENT

The nulling interferometry technique in the infrared is well suited to study any faint cool object located in the immediate environment of a bright astrophysical source (e.g. Voit 1997). A wide range of studies could potentially be conducted using the Darwin-GENIE experiment including infrared spectroscopy of cool dwarfs in spectroscopic binaries, of protoplanetary disks around T Tauri stars, of Herbig Haro objects (Malbet & Bertout 1995) and of Young Stellar Object in general (Kaltenegger et al. 2003). Such programs would be important scientific by-products of the Darwin-GENIE experiment. As an example, a large number of main sequence stars are known to harbor a large quantity of dust. They are mainly early-type stars called Vega type systems after the first discovery of an excess infrared flux around Vega by the satellite IRAS (Aumann et al. 1984). Absil et al. (2003b) simulated observations of a typical Vega-type star ( $\zeta$  Lep) using the GENIE simulation software. The results show that GENIE observations could provide an unprecedented accuracy in the description of the disk morphology including constraints on the dust density and radial temperature distribution. Both the L' and N band could be used for such studies with the VLTI UT telescopes. The auxiliary telescopes that are dedicated to interferometry would also provide valuable information in the L' band. The simulations also show that GENIE could detect disks as faint as 25 times the solar zodiacal cloud brightness around nearby solar type stars. This would allow to prepare the Darwin science program by discarding unsuitable targets for Earth like planet detection by IR nulling interferometry from space (see Sect. 2.2).

Since 1995, more than 100 extrasolar planets have been discovered as companions to solar-type stars (Marcy et al. 2000). All of these planets were discovered indirectly in high-precision Doppler surveys. These surveys measure the radial velocity Doppler shift of the parent star due its periodic motion around the center of mass of the star plus planet system. This technique is most sensitive to massive planets with short orbital periods. The extrasolar planets that have been discovered today have mass ranges from  $M \times \sin i \approx 0.15$  to 10 Jupiter masses (where  $i$  is the orbit inclination onto the observer line of sight) with orbital periods ranging from 3 days to a few years. Because of their proximity to the parent star ( $\ll 1$  AU), the atmosphere of some of these planets is much hotter than that of Jupiter (and of the Earth), hence their name of hot Jupiters. With temperatures sometimes higher than 1000 K, their thermal emission is maximum in the near infrared bands. With baselines ranging from 46 to 130 meters, the VLTI is optimized for the detection in the L band of planets at about 5-15 milli-arcsec from their parent star which correspond to 0.05-0.15 AU for a nearby star at 10 parsecs. This is specially fortunate since these planets are precisely the hot Jupiters of which a significant sample is known. The

contrast between a hot Jupiter and its parent star in the L band is reduced to less than  $10^4$  compared to the  $10^6$  in the N band for Earth-like planets. Den Hartog et al. (2003) simulated an observation of the  $\tau$  Boo system using a GENIE experiment operating in the L' band as a Bracewell interferometer. They found that for the most suitable baseline, the starlight leakage is much higher than the hot-Jupiter signal. They concluded that one major difficulty in the detection of hot Jupiter from ground will be to calibrate the stellar leakage with a high accuracy. One possible solution would be to implement a double-Bracewell configuration (Absil et al. 2002; Gondoin et al. 2003) using internal modulation between two Bracewell nulling interferometers. This configuration could subtract the IR background and the starlight leakage from the overall nulled signal with an accuracy sufficient to retrieve the signal from the brightest exo-Jupiters. The principle of this double Bracewell technique is to recombine the nulled output of two Bracewell interferometers with a  $\pm\pi/2$  phase shift so that new transmission maps are obtained which are asymmetric with respect to the center of the field of view. A maximum of transmission in one map corresponds to a minimum of transmission in the other map. Therefore, an extended source with central symmetry has the same contribution in both outputs. On the other hand, a hot Jupiter located on the maximum of transmission of one map does not give any signal through the other map. Thus, the Jupiter signal can be modulated and therefore retrieved by alternating the two outputs. Although possible in theory, direct detection of the hottest exoplanets on-ground using this nulling interferometry technique in the L' band would be technically more demanding than a single Bracewell interferometer. It is however worth noting that three double-Bracewell configurations are possible at VLTI which offer flexibility in adapting the transmission map to the orbital position of the exo-Jupiters around their parent star.

## 7. CONCLUSION

The Darwin-GENIE nulling experiment will provide European Scientists and Engineers with a first experience on the design, manufacture and operation of a nulling interferometer using Darwin representative concept and technology. Nulling tests on single stars or close binary systems could be achieved in the L' and N atmospheric spectral bands with a nulling rejection ratio higher than a 1000. The Darwin-GENIE experiment will combine all optical functions foreseen into the future Darwin Infrared Space Interferometer. It will demonstrate that nulling interferometry can be achieved in a broad mid-IR band as a precursor to the next phase of the Darwin program.

GENIE is not only a technology demonstrator but also a preparatory experiment for the Darwin science program. The instrument will detect bright exo-zodiacal dust disks around nearby solar type

stars. This would allow to establish the Darwin target list and to discard unsuitable sources for Earth like planet detection from space. Darwin observation scenarios, calibration procedures and data analysis methods will be tested by GENIE. The nulling experiment could also become a very useful instrument for astrophysics that would enable scientist to conduct research programmes on a variety of sources including Herbig Haro and Young Stellar Objects, protoplanetary disks around T Tauri stars, low mass companions and may be hot Jupiters around nearby stars.

## REFERENCES

- Absil O, Gondoin P., den Hartog R., Erd C., Fridlund M., Rando N., 2002, in the Proceedings of La Semaine de l'Astrophysique Francaise, meeting held in Paris, France, June 24-29, 2002, Eds.: F. Combes and D. Barret, EdP-Sciences (Editions de Physique), Conference Series, p. 145
- Absil O, den Hartog R., Erd C., Gondoin P., Kaltenegger L., Fridlund M., Rando N., Wilhelm R., 2003a, in these proceedings.
- Absil O, Kaltenegger L., Eiroa C., den Hartog R., Gondoin P., Fridlund M., Wilhelm R., 2003b, in these proceedings.
- Angel J.R., Cheng A.Y., Woolf N.J., 1986, *Nature* 322, 341
- Backman D.E., Parece F., 1993, in *Protostar and Planet III*, ed. E.H. Levy & J.I. Lunine (Tucson, Univ. of Arizona Press), 1253
- Barillot M., 2004, in these proceedings.
- Bracewell R.N., 1978, *Nature* 274, 780
- den Hartog R., Absil O., Kaltenegger L., Gondoin P., Wilhelm R., Fridlund M., 2003, in these proceedings.
- Eiroa C. et al., 2003, in these proceedings.
- ESA, 2000. Darwin: the Infrared Space Interferometer: Concept and Feasibility Study Report ESA-SCI/2000/12
- Flatscher R., 2003, in these proceedings.
- Fridlund M. 2000, in Proceedings of the Conference 'Darwin and Astronomy - the Infrared Space Interferometer', Stockholm, Sweden, 17-19 November 1999, ESA SP-451
- Fridlund M., Gondoin P. 2003, *SPIE Vol. 4852*, p. 394
- Gondoin P., Absil O., Fridlund M., Erd C., den Hartog R., Rando N., Glindemann A., Koehler B., Wilhelm R., Karlsson A., Labadie L., Mann I., Peacock A., Richichi A., Sodnik Z., Tarenghi M., Volonte S., 2003, *SPIE Vol. 4838*, p. 700
- Kaltenegger L., et al. 2003, in these proceedings.
- Käuff H. U., Bouchet P., Van Dijsseldonk A., Weilenmann U., 1991. *Experimental Astronomy* 2, pp. 115-122
- Kelsall T., Weiland J., Franz B., et al. 1998, *ApJ* 508, 44
- Koresko C. D., Mennesson B. P., Serabyn E., Colavita M., Akeson R. L., Swain M. R., 2003, *Proc. SPIE 4838*, pp. 625-635
- Küchner M. J., Brown M.E., 2000, *PASP* 112, 827
- Leinert C., Graser U., Waters L. B. F. M, Perrin G. S. et al., 2003, *Proc. SPIE 4838*, pp. 893-904
- Malbet F., Bertout C., 1995, *A&AS*, 113, 369
- Marcy G.W., Cochran W.D., Mayor M., 2000, in *Protostar and Planet IV*, ed. V. Mannings, A.P. Boss & S.S. Russel (Tucson, Univ. of Arizona Press), 1285
- Meisner J., Le Poole R., 2003, *Proc. SPIE 4838*, pp. 609-623
- Miyata T. et al. 2000, *Proc. SPIE 4008*, pp. 842-852
- Ollivier M., Mariotti J.M., 1997, *App. Opt.* 36 5340
- Ruilier C., 1998, *Proc. SPIE 3350*, p. 319
- Serabyn E. 2003, in these proceedings.
- Shaklan S., Roddier F., 1988, *App. Opt.* 27, 2334
- Schöller M., Glindemann A., 2003, in these proceedings.
- Voit M. G., 1997, *ApJ* 487, L109
- Wilhelm R., Gitton P., 2003, in these proceedings.